Quantification and characterization of airborne microplastics and their possible hazards: a case study from an urban sprawl in eastern India

Mamun Mandal[1], Anamika Roy[1], Pardeep Singh[2]* and Abhijit Sarkar[1]*

[1]Laboratory of Applied Stress Biology, Department of Botany, University of Gour Banga, Malda, West Bengal, India, [2]Department of Environmental Studies, PGDAV College, University of Delhi, New Delhi, India

One significant way that microplastics (MPs) are transported from the air into soil and water is through deposition. Nevertheless, little is known about the contributing causes and the geographical distribution of MPs in urban air deposition. The present study determined the spatial distribution of MPs and their potential ecological risk in Malda City, West Bengal, India (from December 2023 to February 2024). The average deposition fluxes of MPs were ranging from 122.25 ± 76.96 to 387 ± 89.23 n m^{-2} d^{-1}. Most of the MPs were found in small-sized (50−100 µm) with transparent (35.51%) and white (33.19%) in color. The dominant chemical compositions, such as PE (~32%), PVC (~24%), and PET (~20%), and in the case of shapes such as fragments (~38%) and films (~29%) were the dominant types of MPs found. The geographic heterogeneity seen in the MPs distribution under investigation was mostly caused by human activity and the regions' commercial nature. The MPs deposition fluxes are also affected by rainfall and wind speed. MPs in the deposition may provide a greater ecological concern, according to the early evaluation. According to this study, human activity has a major influence on the source and dispersion of atmospheric MPs that are deposited in urban areas.

1 Introduction

At the early stages of the 21st century, petroleum-based products introduced low molecular-weight monomers to the globe, which resulted in the formation of high molecular-weight organic polymers known as plastics (Mandal et al., 2024a). The manufacture of plastics has grown dramatically, with global output reaching over ~400 million metric tonnes in 2022 (da Costa et al., 2024). Humans find using plastic to be extremely useful and desirable for industrial applications, offering excellent water resistance, high malleability, low degradability, cheap manufacturing costs, and the ability to combine many components for improved performance (Liu et al., 2022). Given that there are over 5,000 distinct varieties of plastic available, a greater quantity of chemicals may be utilized in the production of plastics (da Costa et al., 2024). Most plastic products in this

context are designed to be used once and then promptly disposed off. When it is discharged into the ecosystem, plastic is broken down by photolytic, mechanical, thermal, biological, and chemical processes. It produces small-size plastic polymers such as mega-plastics (>100 mm), macro-plastics (20–100 mm), meso-plastics (5–20 mm), microplastics (MPs; 1 μm-5 mm), and nanoplastics (NPs; 1 nm–1 μm). These are causing a rapid build-up of plastic garbage, and since plastics are more prevalent and persistent in the environment, this leads to environmental problems (Mandal et al., 2024b).

It was recently established that tiny plastic particles, or MPs and NPs, are a common anthropogenic airborne contaminant whose global dispersion and deposition are now predicted (Enyoh et al., 2019; Huang et al., 2020). Furthermore, they are able to move hundreds of kilometers away from their origins due to their tiny size and low weight (Liu et al., 2022). The primary driving factor in the horizontal movement of atmospheric MPs is wind. According to an investigation of air mass trajectories, MPs can travel up to 95 km through the atmosphere (Allen et al., 2019; Loppi et al., 2021). Additional demonstrating research revealed that the atmosphere may carry around 30% of the MPs generated by vehicle traffic to the world's seas (Evangeliou et al., 2020). Between 0.01 m^{-3} in the distant maritime atmosphere (Trainic et al., 2020) to 2,502 m^{-3} at urban roadsides in London, United Kingdom (Levermore et al., 2020), there have been observations of MPs concentrations. Through a hemispheric-scale study, Chen et al. (2023) showed that airborne MPs along a cruise course from the mid-Northern Hemisphere to Antarctica. Most people agree that wet deposition is one of the primary methods by which atmospheric MPs are scavenged (Zhang et al., 2020). However, according to certain research, dry deposition significantly increases the atmospheric MPs fallout (Szewc et al., 2021; Liu et al., 2022).

As MPs are suspended in the atmosphere, they may serve as ice-nucleating particles and/or cloud condensation nuclei, influencing the processes involved in cloud formation. If present in large enough amounts, MPs may alter lifespan, precipitation, and cloud albedo. Taken as a whole, they may have direct radiative impacts that affect Earth's climate by both absorbing and dispersing radiation (Aeschlimann et al., 2022). According to Revell et al. (2021), these consequences were judged to be small, but they have the potential to get worse if waste management and plastic production methods do not improve. Due to their absorption and accumulation in food chains, MPs deposited into aquatic environments, soils, and plants have the potential to harm the ecosystem and human health seriously (Anbumani and Kakkar, 2018; Fang et al., 2022). For example, MPs can be deposited steadily in soil, altering nutrient cycling. They also affect the health of soil fauna (such as nematodes, earthworms and microorganisms) and impact their reproduction, growth, and lifespan (Mandal et al., 2024b).

Since MPs may enter the human body via the respiratory system, direct impacts are also possible. According to prior research (Kernchen et al., 2021), an individual may inhale ~500 MPs particles daily; however, this figure is likely underestimated because only particles smaller than 4 μm were examined. Indeed, human lung tissue obtained during thoracic surgery and autopsy (Amato-Lourenço et al., 2021; Jenner et al., 2022) has been shown to contain MP particles. Studies of the human alveolar cells suggest that airborne MPs may potentially have toxicological consequences on

human health (Goodman et al., 2021). Despite these public concerns, atmospheric MPs are relatively sparsely studied, and more reliable data on MPs levels and behavior in the atmosphere are needed to assess these impacts better.

Keeping the above in mind, the present study has been designed to evaluate the spatial distribution of MPs in the city of Malda, West Bengal, India. Our investigation will advance our knowledge of the MPs dispersion, morphological variances, sources, and possible ecological risks associated with atmospheric MPs deposition in rural, industrial, and urban sprawl. This study provided significant evidence that urban environments and plastic recycling facilities contaminate MPs in the atmosphere. It provided a broad knowledge of how local metrological parameters (such as wind speed and direction, precipitation, etc.), land use patterns (urban, rural and industry, etc.), and population density (densely/scattered) had impacts on MPs distribution. Although there are currently few airborne MPs in the world, this study's findings can close the information gap regarding the amount of emissions in the atmosphere. Furthermore, this study provides a foundation for the advancement of atmospheric MPs monitoring, detection, and mitigation in India in the future. This work contributes to a healthier human environment by assisting in the detection of the hazards associated with exposure to atmospheric MPs pollution, hence addressing SDG 11 indicators.

2 Materials and methods

2.1 Study area and meteorological parameters

The current study investigated in Malda district (West Bengal, India), located in the Eastern Indo-Gangetic plain. Malda is a crucial intersection and point of access to Siliguri from the South side of West Bengal, situated at the meeting point of the Mahananda and Kalindi rivers. Additionally, it is near Bangladesh, which has a 165.5-km international boundary and is a well-known tourist site in West Bengal with a rich history and legacy. However, air pollution in this region has become a growing problem in recent years (Das et al., 2023). Malda's decadal population growth rate (21.2%) is greater than the state average (13.9%) due to its population density of 1,071 inhabitants per km, which is around 4 million (Census of India, 2011). As a result, there is a sharp rise in the area's commercial and residential real estate, roads (there are now two national and one state highway), and vertical and horizontal urban expansion. Nearly 9,350 vehicles per day are estimated to pass over NH-34, according to the National Highway Authority of India (NHAI, 2017; Das et al., 2024). Malda was the epicenter of the thriving cotton and silk factories from the 18th century. Malda is renowned for its mulberries and mangoes. Mango trading and silk production are the region's two primary economic endeavors. In addition, there are a number of small-scale enterprises, including brick kilns, plastic recycling facilities, tobacco factories, food and beverage companies, jute mills and textile factories, and rice mills. So, for this study, we have selected three study sites: Kaliachak (densely populated and has few numbers of plastic recycling facilities), Sujapur where many small plastic recycling facilities are situated, and English Bazar (the main town of national highways, this site is more densely populated than the other sites), to compare the MPs concentration (Figure 1). According to the Census of
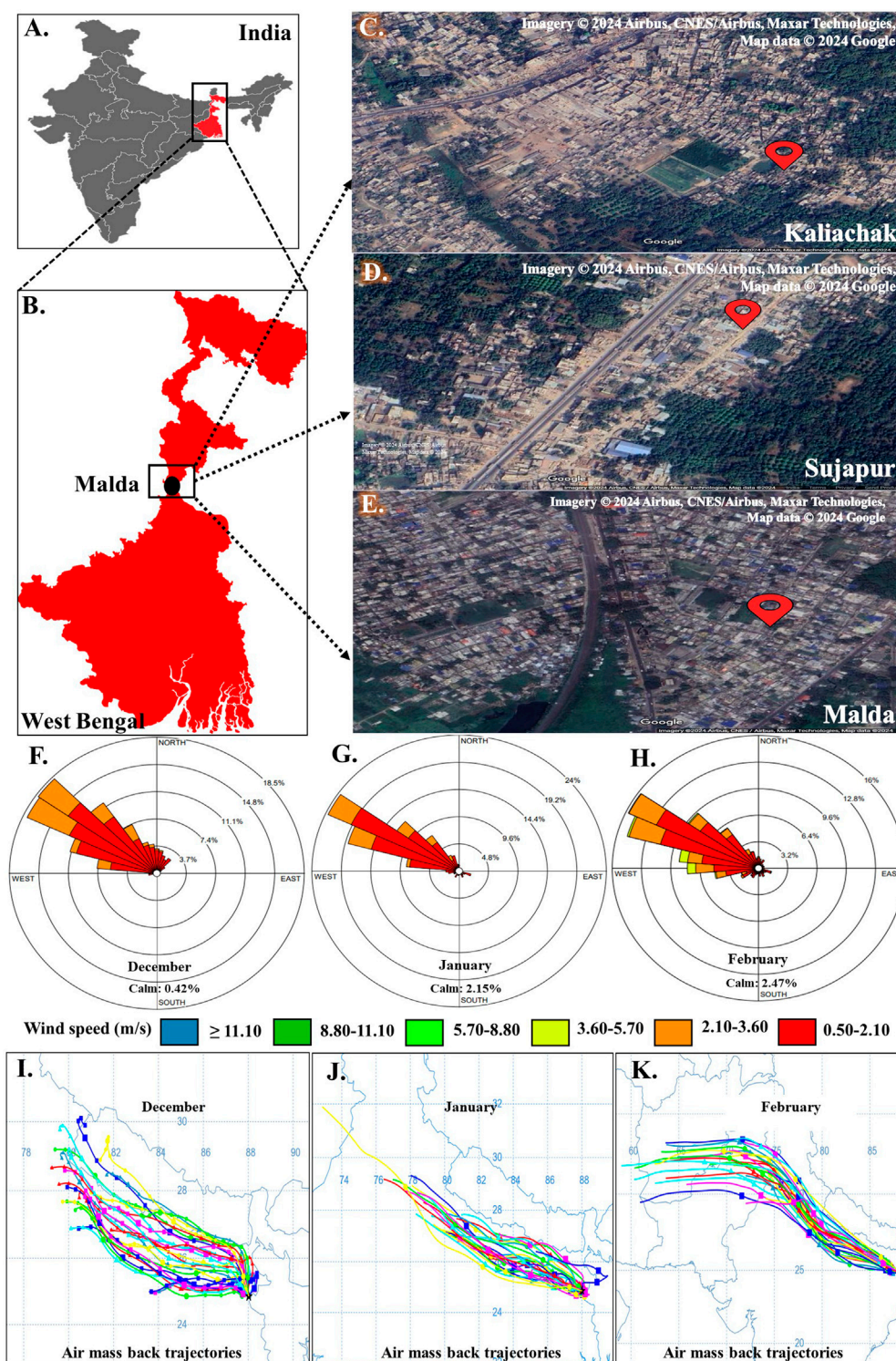
FIGURE 1
Location map of the study area: **(A)** India; **(B)** West Bengal with Malda; **(C)** Sampling site at Kaliachak, Malda; **(D)** Sampling site at Sujapur, Malda; and **(E)** Sampling site at English Bazar, Malda. The wind rose diagram illustrates the wind patterns at the study area for the month of: **(F)** December 2023; **(G)** January 2024; and **(H)** February 2024. Air mass backward trajectory data for the month of-**(I)** December 2023; **(J)** January 2024; and **(K)** February 2024; were obtained using the NOAA HYSPLIT model (https://www.ready.noaa.gov/HYSPLIT.php).

TABLE 1 Meteorological parameters of the study time.

Month	Temperature (°C)	Relative humidity (%)	Precipitation (mm)	Wind speed (m/s)
December 2023	16.77 ± 0.32	78.75 ± 1.01	0.03	1.53 ± 0.08
January 2024	15.23 ± 0.25	71.28 ± 1.45	0.99	1.43 ± 0.06
February 2024	19.57 ± 0.43	57.19 ± 2.86	0.28	1.67 ± 0.11

TABLE 2 The TAD, dry deposition flux of microplastics and its ecological risk assessment of each sampling site.

Sampling sites	TAD (mg m^{-2} d^{-1})	Average dry deposition flux (n m^{-2} d^{-1})	Ecological risk index (RI)	Hazard level
Kalichak (Rural area)	256.30 ± 47.98	122.25 ± 76.96	279.78	Medium
Sujapur (Plastic recycling facility)	345.56 ± 29.56	387.67 ± 89.23	3,535.89	Extreme danger
English Bazar (Roadside Urban area)	479.28 ± 54.90	251.86 ± 108.99	2,467.90	Extreme danger

RI < 150; 150 ≤ RI < 300; 300 ≤ RI < 600; 600 ≤ RI < 1,200; RI ≥ 1,200 (Supplementary Table S1).

India (2011), Kaliachak and Supajur sites are rural types, and the English Bazar area is of an urban nature type.

Data for meteorological studies were recorded using the NASA POWER website (https://power.larc.nasa.gov/). The wind rise plots were made using WRPLOT view ver. 7.0.0 (Lakes Software, Ontario, Canada). The air mass backward trajectories were computed using the Hybrid single-particle Lagrangian Integrated Trajectory (HYSPLIT) model.

2.2 Collection of suspended total atmospheric deposition samples

Suspended total atmospheric deposition (TAD) were collected for the whole study period (December 2023 – February 2024) at every study site using settle glass jars ($n = 3$), which were placed at the height of 3 m above the ground, followed by the Central Pollution Control Board (CPCB) of India and Environmental Protection Agency (EPA) of United States guidelines to maintain distance from pollution sources and anthropogenic interventions, and also to ensure free air circulation. The settle glass jars were cleaned with Milli-Q water before use. To prevent contaminations from insects, large biological waste, and bird droppings, a protective ring was placed at the top of the glass jar (Das et al., 2023). It was calculated using the formula below (Equation 1):

$$\text{TAD } (\text{mg m}^{-2}\text{d}^{-1}) = \text{g particulates} \big/ \text{Ac} \times \text{n} \qquad (1)$$

Here, n is the total number of days the glass jar was exposed, and Ac is the m² cross-sectional area (πr^2) of the glass jar opening.

2.3 Microplastics analyses

2.3.1 Isolation of microplastics

With the use of tweezers, big objects like insects, twigs, and leaves were carefully removed. Particles larger than 5 mm were sieved. For MP analysis, the dust from TAD was utilized. A two-step MP isolation approach was carried out in order to accomplish MP isolation in the ensuing suspended TAD. The 1 gm samples were first processed with 10 mL hydrogen peroxide (30% H_2O_2) in order to eliminate the biogenic organic debris, and they were then kept for 7 days at room temperature (Hengstmann et al., 2018). Next, using the saturated $ZnCl_2$ solution (1.6 g/cm³), MPs were separated by the density flotation. Next, the supernatant was passed through a sieve with pore sizes of 60 μm. Each sample's MPs was obtained three times in total. The $ZnCl_2$ in the filter was rinsed with Milli-Q water for washing, and microsized particles were collected in Petri dishes that were kept in hot air oven dry at 40°C overnight. However, the deposited remaining sample was transferred to triangle flasks for a second-time density separation and treated with 60% NaI (sodium iodide) solution. Then, the same steps were followed and, as soon as possible, the gathered samples were placed in a glass Petri dish and sealed with a matching glass lid. The Petri plates were dehydrated in an oven at 40°C for about 4 h, and then they were refrigerated below 4°C in the dark.

2.3.2 Qualitative analyses of microplastics
2.3.2.1 Stereomicroscope

Physical and rapid documentations of the isolated MPs (300–1,000 μm) were done using stereomicroscope (Model: MX-99). The MPs' shape, color, and size were recorded with the help of an image processing program, ImageJ (Horton et al., 2017). Most of the MPs were white and transparent, which made it difficult to identify them visually (Shim et al., 2016) under the stereomicroscope, so the fluorescent microscope was used for potential confirmation. Because in environmental weathering, the MPs particles started to decolorize.

2.3.2.2 Fluorescent microscope

Nile red (NR) dye, which is a type of lipophilic dye, was used for the fluorescent microscopic (Model: Carl Zeiss, Axioscope 5 FL) documentation of MPs. It exhibits solvatochromic behavior that
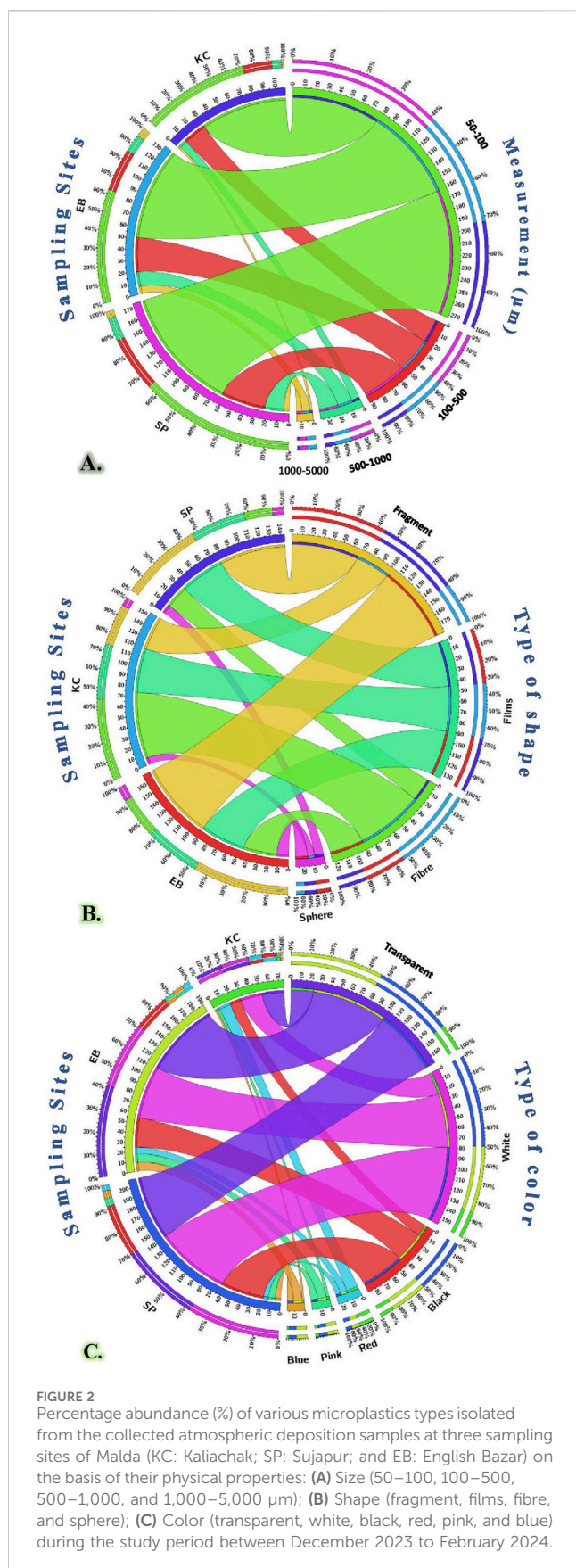
causes fluorescence emission based on the polymer's polarity. Fluorescent microscopy can visualize comparatively smaller range of MPs, and partially identify using fluorescent images when exposed to UV (254–365 nm)/Blue (430–495 nm)/Green (495–570 nm) light. The NR solution was prepared using acetone (0.5 mg/L), and excess dye was rinsed with 200 μL of n-hexane (Yaranal et al., 2021).

2.3.2.3 Chemical fingerprinting of microplastics using fourier transform infrared (FTIR) spectroscopy

Using a Fourier transform infrared spectrometer (FTIR: Model: Thermo Nicolet 5,700), potential MPs were selected and identified. After that, the spectra were examined utilizing the OMNIC spectra library in the OMNIC 9 application (Mecozzi et al., 2016; Veerasingam et al., 2021). The FTIR peaks and graphs were found and drawn respectively generated using OriginPro 9.1. Materials made of plastic were defined as samples with confidence levels greater than 60%. MPs were defined as the range of possible MPs that achieved a quality index higher than 70% (Supplementary Table S1). The study was limited; thus, MPs smaller than 50 μm were not included in the count.

2.4 Deposition fluxes

The described approach was utilized to compute the deposition fluxes of MPs in the samples (Zhou et al., 2017). The following was the equation (Equation 2):

$$\text{Deposition fluxes} \left(\text{n m}^{-2}\,\text{d}^{-1}\right) = \frac{n}{s \times t} \tag{2}$$

Here, t is the sampling interval (d), s is the sample collector's top sectional area (m^2), and n is the number of MPs particles detected per sample (n).
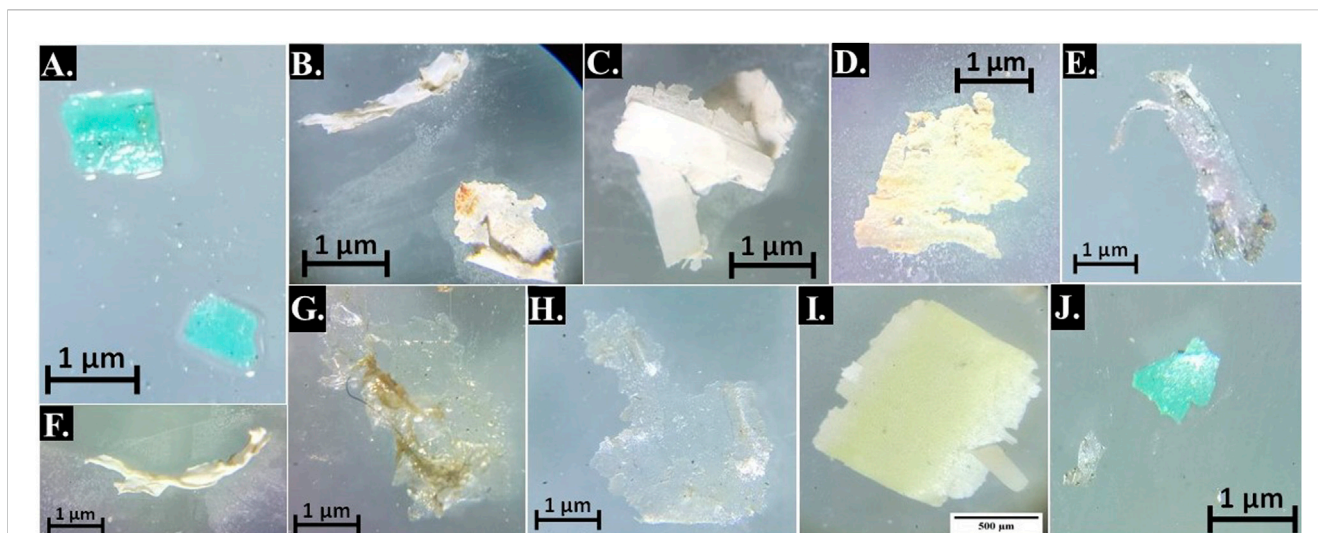
2.5 Potential ecological risk assessment

There is currently no established technique for determining the possible ecological risk associated with MPs. In a recent study by Liu et al., 2022, the ecological risk index (RI) was utilized to evaluate the risk of atmospheric MP (Liu et al., 2019a). Following is the calculation of the RI (Equations 3, 4):

$$RI = \sum_{i=1}^{n} \text{Ei} \tag{3}$$

$$E_i = T_i \times \left(D_i / D_0\right) \tag{4}$$

Here, T_i is the chemical compounds toxicity coefficient (Supplementary Table S2) for polymers as reported by Lithner et al. (2011), D_i is the deposition fluxes (n m^{-2} d^{-1}) of various polymers in each sample, D_0 is the deposition fluxes (n m^{-2} d^{-1}) background, and E_i is the monomial potential ecological risk index. The deposition fluxes (66.04 n m^{-2} d^{-1}) in a area of West Asia were used as the background value due to the lack of such background data on deposition fluxes (Abbasi and Turner, 2021). Hazard level

FIGURE 2
Percentage abundance (%) of various microplastics types isolated from the collected atmospheric deposition samples at three sampling sites of Malda (KC: Kaliachak; SP: Sujapur; and EB: English Bazar) on the basis of their physical properties: **(A)** Size (50−100, 100−500, 500−1,000, and 1,000−5,000 μm); **(B)** Shape (fragment, films, fibre, and sphere); **(C)** Color (transparent, white, black, red, pink, and blue) during the study period between December 2023 to February 2024.

FIGURE 3
Stereomicroscopic documentation of various types of microplastics isolated from different sampling sites during the study period between December 2023 to February 2024. **(A)** fragmented with bluish-green color; **(B, C)** Fragmented with white color; **(D)** Fragmented with white color; **(E)** Fragmented with transparent color; **(F)** Fragmented with white color; **(G, H)** Transparent film; **(I)** Fragmented with white color; and **(J)** Fragmented with bluish-green color. [Identification of the characters were done following Shim et al. (2016)].

was done followed by Liu et al. (2019a) and Hakanson (1980) (Supplementary Table S3). It is crucial to remember that the precise data values were not the main focus of this investigation; rather, they served just as a starting point for more discussion and knowledge on this topic.

2.6 Quality assurance/Quality control

Based on previously published methods, a number of steps were taken to reduce the possibility of contamination (Zhao et al., 2017). To put it briefly, before being used, all sieves, stainless tweezers, and glass jars were wrapped in aluminum foil and baked for four hours at 40°C in a muffle furnace to prevent MPs contamination from undesirable contact/exposure to air contamination. Additionally, every effort was made to minimize the usage of plastic materials. To lessen pollutant residues, plastics that were required for usage were washed with filtered Milli-Q water a minimum of three times. Moreover, nitrile gloves and lab coats made entirely of cotton were worn during the whole sample and processing process. Physical contact with plastic items or equipment was not permitted to avoid contamination during handling and analysis. Finally, after starting the equipment, the experimenters departed the instrument location right away and kept a distance of around 40–50 m downwind for sampling (Liu et al., 2019a). During analysis and identification, laboratory blanks were used to evaluate MPs contamination, and the findings were eliminated for self-contamination.

2.7 Statistical analyses

Microsoft Excel (2019) was utilized for organizing and analyzing the MPs identification data. After evaluating the

blank samples independently, the average number of MPs was deducted from the atmospheric sample data. The 'chorddiag' package in R software (v3.6.1) was utilized to create the "Chord" diagrams for the analyses of different types (color, size, and shape) of MPs abundance (%) and MPs in different locations. Similarly, the "ggplot2" tool in R software was utilized to create the "Sankey diagram" for the analyses of polymer abundance (%) in different locations.

3 Results and discussion

3.1 Meteorological condition at the time of study

The study was carried out during the post-monsoon season, with an average temperature of 17.19°C ± 0.29°C and a relative humidity of 69.1% ± 1.37% throughout the study period (December-February). The average precipitation was 0.43 mm during the study period. Monthly average data are presented in Table 1. The average wind speed was 1.53 m/s with 1.95% of calm days. Most of the wind was dominated by the northwest during the study period, as shown in the wind rose plot (Figure 1). Meteorological conditions have a significant impact on the air quality of the urban agglomeration (Pérez et al., 2020). In general, lower wind speed can hinder the dispersion of air pollutants and reduce the vertical dispersion, which influences PM more likely to be trapped within the restricted mixing layer, thus aggravating the concentration of contaminants (Das et al., 2023). The study period was characterized by lower temperature, medium-to-high humidity, low wind speed, and minimal precipitation, which significantly increased the escalation of the pollutants' concentration in the atmosphere (Table 1). Furthermore, the complex topography and land-use patterns of urbanized areas
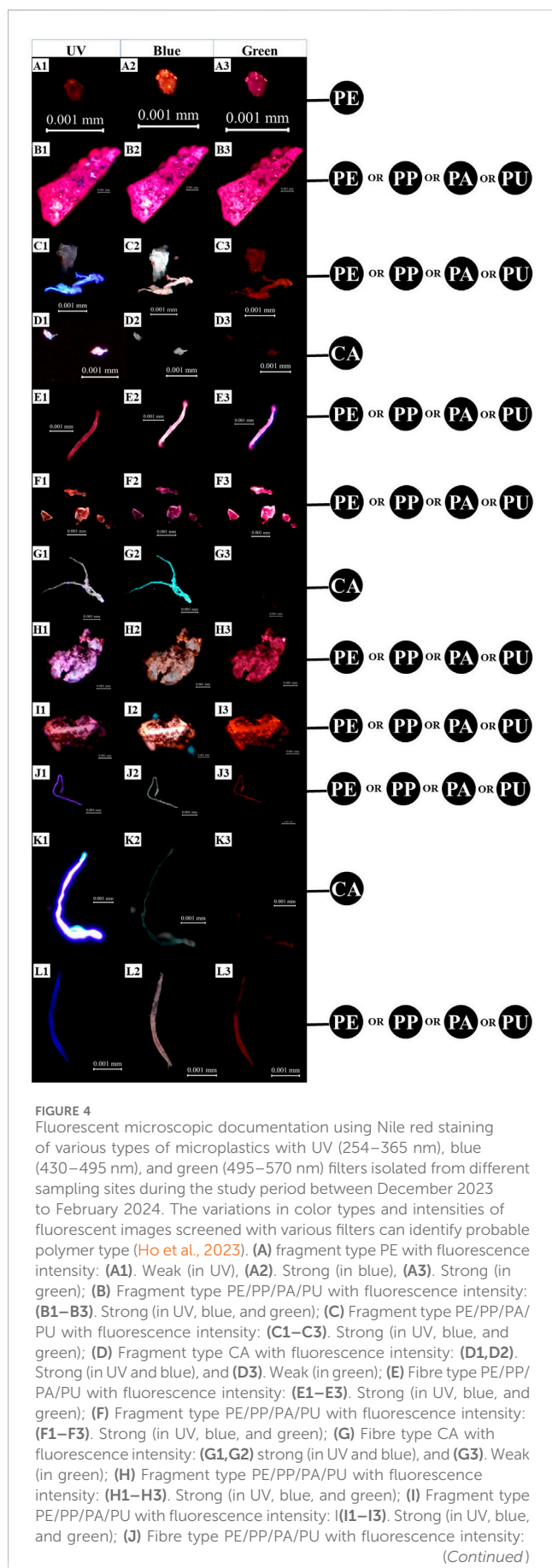
FIGURE 4
Fluorescent microscopic documentation using Nile red staining of various types of microplastics with UV (254−365 nm), blue (430−495 nm), and green (495−570 nm) filters isolated from different sampling sites during the study period between December 2023 to February 2024. The variations in color types and intensities of fluorescent images screened with various filters can identify probable polymer type (Ho et al., 2023). **(A)** fragment type PE with fluorescence intensity: **(A1)**. Weak (in UV), **(A2)**. Strong (in blue), **(A3)**. Strong (in green); **(B)** Fragment type PE/PP/PA/PU with fluorescence intensity: **(B1−B3)**. Strong (in UV, blue, and green); **(C)** Fragment type PE/PP/PA/PU with fluorescence intensity: **(C1−C3)**. Strong (in UV, blue, and green); **(D)** Fragment type CA with fluorescence intensity: **(D1,D2)**. Strong (in UV and blue), and **(D3)**. Weak (in green); **(E)** Fibre type PE/PP/PA/PU with fluorescence intensity: **(E1−E3)**. Strong (in UV, blue, and green); **(F)** Fragment type PE/PP/PA/PU with fluorescence intensity: **(F1−F3)**. Strong (in UV, blue, and green); **(G)** Fibre type CA with fluorescence intensity: **(G1,G2)** strong (in UV and blue), and **(G3)**. Weak (in green); **(H)** Fragment type PE/PP/PA/PU with fluorescence intensity: **(H1−H3)**. Strong (in UV, blue, and green); **(I)** Fragment type PE/PP/PA/PU with fluorescence intensity: I**(I1−I3)**. Strong (in UV, blue, and green); **(J)** Fibre type PE/PP/PA/PU with fluorescence intensity:
(*Continued*)

FIGURE 4 (Continued)
(J1−J3). Strong (in UV, blue, and green); **(K)** Fibre type CA with fluorescence intensity: **(K1,K2)**. Strong (in UV and blue), and **(K3)**. Weak (in green); **(L)** Fibre type PE/PP/PA/PU with fluorescence intensity: **(L1−L3)**. Strong (in UV, blue, and green). The polymer types are PA, polyamide; PP, polypropylene; PE, polyethylene; PU, polyurethane; CA, Cellulose acetate.

can create internal boundary layers and hinder intricate wind flow, exacerbating the impact (Murthy et al., 2020). For example, the studied area of Malda city is a densely populated city (such as the English Bazar area) and the industrialized regions (such as the plastic recycling area, Sujapur).

The (Hybrid Single Particle Lagrangian Integrated Trajectory) HYSPLIT model was used to compute air mass backward trajectories at Malda throughout the study period. Backward trajectory data was obtained from the Air Resource Laboratory (ARL) datasets under the National Oceanic and Atmospheric Administration (NOAA) (https://www.ready.noaa.gov/HYSPLIT.php). The HYSPLIT was used to generate 72-h backward trajectories at various altitudes above ground level (AGL) for the sampling period, highlighting the origin of air pollutants at the study site. The analysis revealed that the air mass reached Malda from Lucknow, Bihar, Jharkhand, Nepal, and Uttarakhand in December, from Pakistan, Haryana, New Delhi, Bihar, Uttar Pradesh in January, and from Uttar Pradesh, Pakistan, and Afghanistan in February (Figure 1).

3.2 Spatial distribution of microplastics in the atmospheric deposition

The TAD was higher in the English Bazar site (479.28 ± 54.9 mg m^{-2}d^{-1}), but the total dry deposition flux of MPs was higher in the Sujapur plastic recycling facility region (387.67 ± 89.23 n m^{-2} d^{-1}). The average total deposition fluxes of Kaliachak, English Bazar, and Sujapur areas were 122.25 ± 76.96, 251.86 ± 108.99, and 387.67 ± 89.23 n m^{-2} d^{-1}, respectively (Table 2). In contrast, urbanized coastal zone of the Gulf of Gdansk (Poland) (Szewc et al., 2021), there are deposition fluxes of 10 ± 8 m^{-2} d^{-1}, which was lower than all the study sites, which may be due to the local MPs pollution sources (plastic recycling factories, tire wear, highways, waste) higher in this study areas. Whereas, in central London, there are fluxes of 771 ± 167 m^{-2} d^{-1} (Wright et al., 2020), which was higher than the studied areas. The tendency towards variety was in line with the shift in human activities. For example, in megacities, changing human consumption patterns, daily lifestyle, and single-time product use habits (such as plastic bottles and food rap) are all responsible for significantly influencing the solid waste that tremendously induces MPs in the environment (Loppi et al., 2021; Mandal et al., 2024a; Mandal et al., 2024c). Given that the MPs in the deposition were found to originate from nearby sources, human activity may have a significant role in affecting the production of MPs (Fu et al., 2020). The number of MPs declined in rural regions (Kaliachak) due to a reduction in human activity, which may have been aided by garbage disposal and local markets. On the other hand, the Sujapur area is also a rural type, but due to plastic recycling facilities, the MPs deposition fluxes was higher than in the urban area (English Bazar). This was
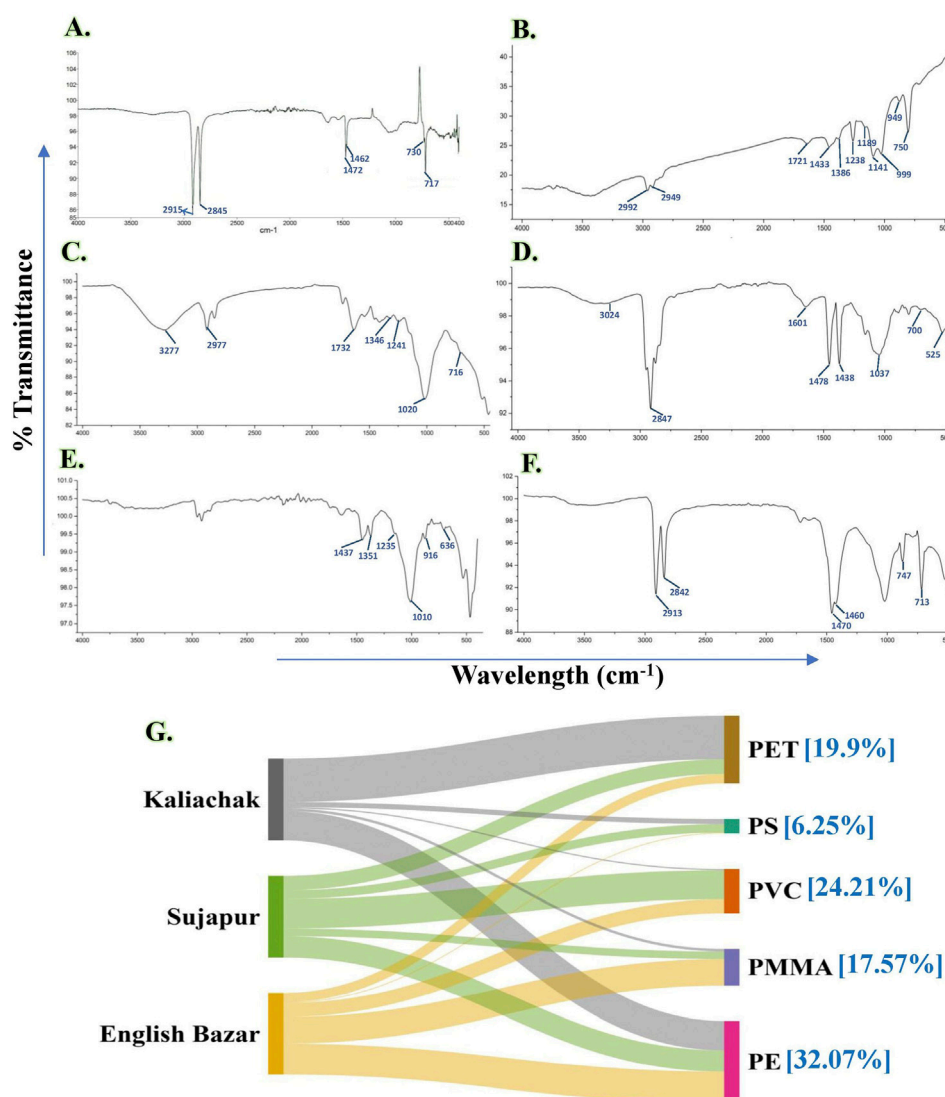
FIGURE 5
Fourier Transform Infrared spectroscopy (FTIR) spectra and combined percentage of polymer abundance of various microplastics isolated from different sampling sites during the study period between December 2023 to February 2024. FTIR spectrum identified for individual polymer type: **(A)** Polyethylene (PE); **(B)** Polymethyl methacrylate (PMMA); **(C)** Polyethylene terephthalate (PET); **(D)** Polystyrene (PS); **(E)** Polyvinyl chloride (PVC); **(F)** PE. **(G)** Combined percentage of polymer abundance among study sites calculated using all the FTIR spectra together are represented through Sankey diagram ("ggplot2" tool in R software v3.6.1).

confirmed in many locations by the distribution area of abundant MPs. Therefore, the increased release of MPs from regional sources into the atmosphere was caused by changes in human activity and the character of local commerce (Allen et al., 2019).

However, higher population density and commercial nature (plastic recycling factories, textile factories) of the area are also important factors like human activity (national highways and vehicles) that increase the MPs intensity in the two function zones (English Bazar and Sujapur) more than the rural/remote areas (i.e., Kaliachak) (Dris et al., 2017). Our findings supported earlier studies that demonstrated deposition fluxes in densely inhabited urban regions were much greater than those in sparsely populated suburban areas (Dris et al., 2016).

However, wind speed also significantly influences the deposition fluxes of MPs; for example, higher wind speed (20.5–23.5 m/s) induces the dispersion of MPs, but the lower rate of wind speed increases the local deposition fluxes of MPs (van der Does et al., 2018). MPs can remain suspended in the atmosphere for weeks before being carried by the wind (van der Does et al., 2018). On the other hand, precipitation might influence the atmospheric deposition of MPs (Dris et al., 2015; Dris et al., 2016; Allen et al., 2019). A higher abundance of MPs presence indicated that rainfall and wind speed were the major natural factors in deposition. In this study, throughout the three-month of MPs collection period, it was lower, ranging from 1.43 ± 0.06 m/s to 1.67 ± 0.11 m/s. So, from this result, it can be predicted that the lower range of wind may be the

reason for MPs fluxes in study areas. Likewise, there were significantly fewer deposition fluxes in rural regions of Kaliachak, which may be due to wind speed, which will be determined in future studies. Similarly, precipitation was very low at the time of study, ranging from 0.03 to 0.99 mm, so MPs particles in the atmosphere can not be effectively scavenged by the wind and dispersed (Li et al., 2020).

Based on the long-range transit study of MPs, it was also proposed that the urban area itself served as the center of influence for deposited MPs in central London (Wright et al., 2020). So, in this study, we found that in Malda city, air mass came from different states (Lucknow, Bihar, Jharkhand, Nepal, and Uttarakhand in December, from Haryana, New Delhi, Bihar, Uttar Pradesh in January, and from Uttar Pradesh in February) as well as from other countries (Pakistan, and Afghanistan). We concluded that maybe the MPs also came from these regions. Because, wind may have a significant impact on the geographical distribution of deposited MPs, according to the various deposition fluxes observed in the valley basin city (Li et al., 2020). Considering the preceding, it can be concluded from the above statements that both natural and human influences influenced the MPs' geographical distribution during deposition.

3.3 Physico-chemical characterization of isolated microplastics

According to Zhang et al. (2020), atmospheric MPs are typically smaller than water and terrestrial environments. Likewise, in this study in all the sampling locations, the majority of MPs (~70%) had sizes between 50 and 500 μm; this matched findings from other research (Zhou et al., 2017; Bergmann et al., 2019). Small-size (50–100 μm) MPs were predominant in every sampling site size, followed by medium-size (100–1,000 μm) and large-size (1,000–5,000 μm) MPs. According to monitoring data from remote places, most MPs in deposition had diameters of less than 50 μm (Allen et al., 2019; Bergmann et al., 2019). This implied that long-distance transport was far more likely to be accomplished by the smaller MPs (Hüffer et al., 2019). It had been shown that dry and wet deposition accounted for the majority of the removal of larger-diameter air particles. Long-distance airflow transportation proved difficult for them (Dai, 2006; Mandal et al., 2023; Roy et al., 2024). Therefore, MPs in the deposition samples that were obtained may originate locally rather than elsewhere. The main colors of MPs were transparent (35.51%) and white (33.19%), followed by black (18.6%), red (5%), pink (4.01%), and blue (3.59%). Transparent and white MPs comprised ~69% of the population, which was the highest proportion (Figure 2). In Figures 3, 4, we have added the stereomicroscope and fluorescent images, respectively, that represent different kinds of MPs diversity in the samples. These results depicted that MPs' color may be bleached or affected by abiotic (such as sunlight-induced photooxidation or weathering, moisture, dryness, temperature, etc.) and biotic (such as microbial deterioration, etc.) factors in the environment that can increase the number of light-colored MPs (Mandal et al., 2024a). In the case of the shape, MPs were fragments (38.41%), and films (28.96%) were the most dominant type, followed by fibre (26.6%) and spheres (6%).

MPs particles, particularly fibres, have the ability to penetrate both adult and pediatric lung membranes because of their smaller size, which can result in respiratory diseases and inflammation (Prata, 2018; Yurtsever et al., 2018). Moreover, toxic materials such as infections, trace metals, and persistent organic pollutants can attach to MPs and enter the body, weakening the immune system (Lambert et al., 2017).

The fluorescent properties of MPs differed greatly according to surface structure (viz. weathered), color, shape, and polymer density (Prata et al., 2019). However, NR fluorescent intensity differed significantly between polar (viz. PET, nylon) and hydrophobic (PP, PE, PS) groups of polymers (Figure 4). Based on that, we have classified the probable polymer type, followed by Ho et al. (2023) library construction that depicts their fluorescence intensity under different filters. While PTFE and PMMA MPs did not respond stereotypically to NR-stained, their limited response renders them undetected using fluorescent imaging (Capolungo et al., 2021). The fluorescence was observed for the majority of MPs across UV and blue wavelengths (Figure 4). Contradictorily, many studies preferred using green light fluorescent over UV and blue light to improve the detectability of NR-stained samples (Sturm et al., 2021). PE, PP, PU, and nylon (PA) showed strong fluorescent brightly against UV, blue, and green filters (Ho et al., 2023). Additionally, if the fluorescent intensity was high on UV and green filers but low in blue filters, it was supposed to be PE and PET. If any MPs were strongly fluorescent in the UV and blue light, it was considered a cellulose acetate (CA) polymer type. At the same time, we could not identify many kinds of MPs. This is mainly because field investigations are limited to estimating the number of MPs and hence fail to analyze and provide evident knowledge of the NR fluorescence color of all polymer types after excitation and emission (Shruti et al., 2022; Ho et al., 2023). In this case, spectroscopic techniques such as FTIR have often been employed to determine the polymer composition (Figure 5).

3.4 Identification of specific polymer in isolated microplastics using FTIR spectra

Five kinds of MP polymers were found by FTIR analysis: PE (32.07%), PVC (24.21%), PET (19.9%), PMMA (17.57%), and PS (6.25%) (Figure 5). Its specific polymer characteristics and range may aid in determining its origins. For example, the presence of PE-type polymer indicates that it may come from packing/rapping or other type single-use materials; likewise, the presence of PET-type polymer suggests that it came from water bottles or synthetic clothing fiber (Rodríguez-Seijo and Pereira, 2017). According to several studies, PVC and PE make up the majority of MPs in urban deposition and are the primary constituents of films and fragments, respectively (Zhou et al., 2017; Klein and Fischer, 2019). The various MPs sources (such as pipes, soda and water bottles, plastic bags, fishing nets, tea bags, microwave containers, cigarette buds, tire and road wear particles) in the multiple cities might explain this. PMMA is a unique polymer type of urban atmospheric plastics, as demonstrated by earlier research, which may be related to transportation intersections because, due to its durability and lightweight, it has been used for tire industries. Additionally, it is generally used in light boxes, wall posters, frames, containers, and

microbeads in the cosmetics industry. A recent investigation on MPs in a Shanghai waste glass recycling facility revealed a significant amount of PMMA in the dust (Zhang et al., 2021). The PET (18.14%), PE (26.20%), and PVC (35.88%) in plastic recycling centers showed the most significant proportion.

4 Ecological risk assessment

The ranges of RI in the three areas were 279.78, 3,535.89, and 2,467.90, Kalichak, Sujapur, and English Bazar, respectively (Table 2). This result indicated that Sujapur and English Bazar are prone to extreme danger levels. According to other studies employing a comparable evaluation technique, there was no danger associated with suspended atmospheric MPs (Liu et al., 2019a). However, in our investigation, atmospheric MPs are significantly associated with the medium to extreme level of hazard. Furthermore, the greater Ei of PMMA and PVC—both of which have high chemical toxicity coefficients—was principally responsible for the higher RI. The risk level in the major town (English Bazar) and plastic recycling in Sujapur was quite high. The greater PVC deposition fluxes in this region explained this. Of the five polymer kinds, only the monomial risk ratings of PVC and PMMA were severely harmful. Because, PVC polymer is a type of organochlorine compound that is more toxic than other chlorine-containing MPs polymer. When PVC-MPs are exposed to higher-intensity light, they emit organotin chemicals such as monobutyltin, dibutyltin, monomethyltin and dimethyltin, which are carcinogenic (Nosova and Uspenskaya, 2023). Similarly, PMMA exposed to high temperatures in the environment can produce toxic gases like carbon dioxide, carbon monoxide, and organic compounds. Methyl methacrylate is the main monomer of PMMA, which causes allergic reactions, especially for those with weak skin sensitivities; additionally, it can induce thermal damages to neural tissues (Pikis et al., 2015). The chemical toxicity coefficient of plastic polymers (Lithner et al., 2011) was utilized in place of the usual toxic-response factor (Ti) for plastic polymers in prospective ecological risk assessment. The estimation of the possible ecological risk of MPs in deposition may have been overstated because the chemical toxicity coefficient was the plastic polymers' maximum degree of hazard. However, in the lack of adequate information regarding the physiological toxicity of MPs, the evaluation results continued to have reference value when investigating the ecotoxicity of air MPs.

5 Conclusion

For the first time, the geographical distribution (such as recycling factories, urban and rural areas) and the possible ecological risk of MPs in Malda City's atmospheric deposition were examined in this study. The dominant MPs samples were mostly composed of white and transparent in case of color, while PE, PVC, and PET were in polymer type. The small size (50–100 μm) fragmented and films types of MPs were the most abundant types. Both the urban area (English Bazar) and plastic recycling facility area (Sujapur) had 'extreme danger' levels of ecological risk, whereas the rural area (Kaliachak) had the 'medium' level of ecological risk.

There was spatial variance in the MPs distribution in the deposition. The primary factors influencing the geographical distribution of MPs in deposition were human activity and plastic recycling facilities. Additionally, the low amount of rainfall and wind speed had an impact on MPs distribution. However, more researches on atmospheric MPs deposition are required to offer any general standard methodology for locating MPs sources and evaluating the possible ecological risk caused by MPs. Even, the limited availability of the polymer database might create a hindrance or biasness for specific identification. According to present literature, very little data are available on human exposure and further health hazards. So, with more available data, the present ecological indices might vary regarding the risk and hazard levels. The dry deposition fluxes of atmospheric MPs might vary with seasonal meteorological and source variations. More detailed studies would definitely help to better conclude, and project map regarding the MPs population and hazard/risk dynamics.

Data availability statement

The raw data supporting the conclusions of this article will be made available by the authors, without undue reservation.

Author contributions

MM: Data curation, Formal Analysis, Investigation, Methodology, Visualization, Writing–original draft. AR: Formal Analysis, Writing–review and editing. PS: Conceptualization, Supervision, Writing–review and editing. AS: Conceptualization, Data curation, Methodology, Supervision, Writing–review and editing.

Conflict of interest

The authors declare that the research was conducted in the absence of any commercial or financial relationships that could be construed as a potential conflict of interest.

Publisher's note

All claims expressed in this article are solely those of the authors and do not necessarily represent those of their affiliated organizations, or those of the publisher, the editors and the reviewers. Any product that may be evaluated in this article, or claim that may be made by its manufacturer, is not guaranteed or endorsed by the publisher.

Supplementary material

The Supplementary Material for this article can be found online at: https://www.frontiersin.org/articles/10.3389/fenvc.2024.1499873/full#supplementary-material

References

Abbasi, S., and Turner, A. (2021). Dry and wet deposition of microplastics in a semi-arid region (Shiraz, Iran). *Sci. Total Environ.* 786, 147358. doi:10.1016/j.scitotenv.2021.147358

Aeschlimann, M., Li, G., Kanji, Z. A., and Mitrano, D. M. (2022). Potential impacts of atmospheric microplastics and nanoplastics on cloud formation processes. *Nat. Geosci.* 15 (12), 967–975. doi:10.1038/s41561-022-01051-9

Allen, S., Allen, D., Phoenix, V. R., Le Roux, G., Durántez Jiménez, P., Simonneau, A., et al. (2019). Atmospheric transport and deposition of microplastics in a remote mountain catchment. *Nat. Geosci.* 12 (5), 339–344. doi:10.1038/s41561-019-0335-5

Amato-Lourenço, L. F., Carvalho-Oliveira, R., Júnior, G. R., dos Santos Galvão, L., Ando, R. A., and Mauad, T. (2021). Presence of airborne microplastics in human lung tissue. *J. Hazard. Mater.* 416, 126124. doi:10.1016/j.jhazmat.2021.126124

Anbumani, S., and Kakkar, P. (2018). Ecotoxicological effects of microplastics on biota: a review. *Environ. Sci. Pollut. Res.* 25, 14373–14396. doi:10.1007/s11356-018-1999-x

Bergmann, M., Mützel, S., Primpke, S., Tekman, M. B., Trachsel, J., and Gerdts, G. (2019). White and wonderful? Microplastics prevail in snow from the Alps to the Arctic. *Sci. Adv.* 5 (8), eaax1157. doi:10.1126/sciadv.aax1157

Capolungo, C., Genovese, D., Montalti, M., Rampazzo, E., Zaccheroni, N., and Prodi, L. (2021). Photoluminescence-based techniques for the detection of micro- and nanoplastics. *Chemistry–A Eur. J.* 27 (70), 17529–17541. doi:10.1002/chem.202102692

Census of India (2011). *Ministry of home affairs, government of India*. Available at: https://censusindia.gov.in/2011census/PCA/A4.html (Accessed February 12, 2023).

Chen, Q., Shi, G., Revell, L. E., Zhang, J., Zuo, C., Wang, D., et al. (2023). Long-range atmospheric transport of microplastics across the southern hemisphere. *Nat. Commun.* 14 (1), 7898. doi:10.1038/s41467-023-43695-0

da Costa, M. B., Schuab, J. M., dos Santos Sad, C. M., Ocaris, E. R. Y., Otegui, M. B. P., Motta, D. G., et al. (2024). Microplastic atmospheric pollution in an urban Southern Brazil region: what can spider webs tell us? *J. Hazard. Mater.* 477, 135190. doi:10.1016/j.jhazmat.2024.135190

Dai, S. (2006). *Environmental chemistry*. Beijing, China: China Higher Education Press.

Das, S., Barman, C., Roy, A., Mandal, M., Popek, R., Adit, A., et al. (2024). Air pollution may alter reproductive dynamics/efficacy in plants: correlative evidences from an urban sprawl in Eastern Indo-Gangetic plain. *Aerobiologia*, 1–19. doi:10.1007/s10453-024-09811-3

Das, S., Roy, A., Masiwal, R., Mandal, M., Popek, R., Chakraborty, M., et al. (2023). Comprehensive analysis of PM_1 composition in the eastern indo-gangetic basin: a three-year urban study. *Sustainability* 15, 14894. doi:10.3390/su152014894

Dris, R., Gasperi, J., Mirande, C., Mandin, C., Guerrouache, M., Langlois, V., et al. (2017). A first overview of textile fibers, including microplastics, in indoor and outdoor environments. *Environ. Pollut.* 221, 453–458. doi:10.1016/j.envpol.2016.12.013

Dris, R., Gasperi, J., Rocher, V., Saad, M., Renault, N., and Tassin, B. (2015). Microplastic contamination in an urban area: a case study in Greater Paris. *Environ. Chem.* 12 (5), 592–599. doi:10.1071/en14167

Dris, R., Gasperi, J., Saad, M., Mirande, C., and Tassin, B. (2016). Synthetic fibers in atmospheric fallout: a source of microplastics in the environment? *Mar. Pollut. Bull.* 104 (1–2), 290–293. doi:10.1016/j.marpolbul.2016.01.006

Enyoh, C. E., Verla, A. W., Verla, E. N., Ibe, F. C., and Amaobi, C. E. (2019). Airborne microplastics: a review study on method for analysis, occurrence, movement and risks. *Environ. Monit. Assess.* 191 (11), 668. doi:10.1007/s10661-019-7842-0

Evangeliou, N., Grythe, H., Klimont, Z., Heyes, C., Eckhardt, S., Lopez-Aparicio, S., et al. (2020). Atmospheric transport is a major pathway of microplastics to remote regions. *Nat. Commun.* 11 (1), 3381. doi:10.1038/s41467-020-17201-9

Fang, M., Liao, Z., Ji, X., Zhu, X., Wang, Z., Lu, C., et al. (2022). Microplastic ingestion from atmospheric deposition during dining/drinking activities. *J. Hazard. Mater.* 432, 128674. doi:10.1016/j.jhazmat.2022.128674

Fu, D., Chen, C. M., Qi, H., Fan, Z., Wang, Z., Peng, L., et al. (2020). Occurrences and distribution of microplastic pollution and the control measures in China. *Mar. Pollut. Bull.* 153, 110963. doi:10.1016/j.marpolbul.2020.110963

Goodman, K. E., Hare, J. T., Khamis, Z. I., Hua, T., and Sang, Q. X. A. (2021). Exposure of human lung cells to polystyrene microplastics significantly retards cell proliferation and triggers morphological changes. *Chem. Res. Toxicol.* 34 (4), 1069–1081. doi:10.1021/acs.chemrestox.0c00486

Hakanson, L. (1980). An ecological risk index for aquatic pollution control. A sedimentological approach. *Water Res.* 14 (8), 975–1001. doi:10.1016/0043-1354(80)90143-8

Hengstmann, E., Tamminga, M., vom Bruch, C., and Fischer, E. K. (2018). Microplastic in beach sediments of the Isle of Rügen (Baltic Sea) - implementing a novel glass elutriation column. *Mar. Pollut. Bull.* 126, 263–274. doi:10.1016/j.marpolbul.2017.11.010

Ho, D., Liu, S., Wei, H., and Karthikeyan, K. G. (2023). The glowing potential of Nile red for microplastics Identification: Science and mechanism of fluorescence staining. *Microchem. J.* 197, 109708. doi:10.1016/j.microc.2023.109708

Horton, A. A., Walton, A., Spurgeon, D. J., Lahive, E., and Svendsen, C. (2017). Microplastics in freshwater and terrestrial environments: evaluating the current understanding to identify the knowledge gaps and future research priorities. *Sci. total Environ.* 586, 127–141. doi:10.1016/j.scitotenv.2017.01.190

Huang, Y., Qing, X., Wang, W., Han, G., and Wang, J. (2020). Mini-review on current studies of airborne microplastics: analytical methods, occurrence, sources, fate and potential risk to human beings. *TrAC Trends Anal. Chem.* 125, 115821. doi:10.1016/j.trac.2020.115821

Hüffer, T., Metzelder, F., Sigmund, G., Slawek, S., Schmidt, T. C., and Hofmann, T. (2019). Polyethylene microplastics influence the transport of organic contaminants in soil. *Sci. Total Environ.* 657, 242–247. doi:10.1016/j.scitotenv.2018.12.047

Jenner, L. C., Rotchell, J. M., Bennett, R. T., Cowen, M., Tentzeris, V., and Sadofsky, L. R. (2022). Detection of microplastics in human lung tissue using µFTIR spectroscopy. *Sci. Total Environ.* 831, 154907. doi:10.1016/j.scitotenv.2022.154907

Kernchen, S., L̈oder, M., Fischer, F., Fischer, D., Moses, S., and Georgi, C. (2021). Airborne microplastic concentrations and deposition across the Weser river catchment. *Sci. Total Environ.* 818, 151812. doi:10.1016/j.scitotenv.2021.151812

Klein, M., and Fischer, E. K. (2019). Microplastic abundance in atmospheric deposition within the Metropolitan area of Hamburg, Germany. *Sci. Total Environ.* 685, 96–103. doi:10.1016/j.scitotenv.2019.05.405

Lambert, S., Scherer, C., and Wagner, M. (2017). Ecotoxicity testing of microplastics: considering the heterogeneity of physicochemical properties. *Integr. Environ. Assess. Manag.* 13 (3), 470–475. doi:10.1002/ieam.1901

Levermore, J. M., Smith, T. E., Kelly, F. J., and Wright, S. L. (2020). Detection of microplastics in ambient particulate matter using Raman spectral imaging and chemometric analysis. *Anal. Chem.* 92 (13), 8732–8740. doi:10.1021/acs.analchem.9b05445

Li, X., Wang, J., Eftekhari, M., Qi, Q., Jiang, D., Song, Y., et al. (2020). Improvement strategies study for outdoor wind environment in a university in Beijing based on CFD simulation. *Adv. Civ. Eng.* 2020 (1), 8850254. doi:10.1155/2020/8850254

Lithner, D., Larsson, Å., and Dave, G. (2011). Environmental and health hazard ranking and assessment of plastic polymers based on chemical composition. *Sci. total Environ.* 409 (18), 3309–3324. doi:10.1016/j.scitotenv.2011.04.038

Liu, K., Wang, X., Fang, T., Xu, P., Zhu, L., and Li, D. (2019a). Source and potential risk assessment of suspended atmospheric microplastics in Shanghai. *Sci. Total Environ.* 675, 462–471. doi:10.1016/j.scitotenv.2019.04.110

Liu, Z., Bai, Y., Ma, T., Liu, X., Wei, H., Meng, H., et al. (2022). Distribution and possible sources of atmospheric microplastic deposition in a valley basin city (Lanzhou, China). *Ecotoxicol. Environ. Saf.* 233, 113353. doi:10.1016/j.ecoenv.2022.113353

Loppi, S., Roblin, B., Paoli, L., and Aherne, J. (2021). Accumulation of airborne microplastics in lichens from a landfill dumping site (Italy). *Sci. Rep.* 11, 4564. doi:10.1038/s41598-021-84251-4

Mandal, M., Popek, R., Przybysz, A., Roy, A., Das, S., and Sarkar, A. (2023). Breathing fresh air in the city: implementing avenue trees as a sustainable solution to reduce particulate pollution in urban agglomerations. *Plants* 12 (7), 1545. doi:10.3390/plants12071545

Mandal, M., Roy, A., Das, S., Rakwal, R., Agrawal, G. K., Singh, P., et al. (2024c). Food waste-based bio-fertilizers production by bio-based fermenters and their potential impact on the environment. *Chemosphere* 141539.

Mandal, M., Roy, A., Mitra, D., and Sarkar, A. (2024a). Possibilities and prospects of bioplastics production from agri-waste using bacterial communities: finding a silver-lining in waste management. *Curr. Res. Microb. Sci.* 7, 100274. doi:10.1016/j.crmicr.2024.100274

Mandal, M., Roy, A., Popek, R., and Sarkar, A. (2024b). Micro-and nano-plastic degradation by bacterial enzymes: a solution to 'white pollution. *Microbe* 3, 100072. doi:10.1016/j.microb.2024.100072

Mecozzi, M., Pietroletti, M., and Monakhova, Y. B. (2016). FTIR spectroscopy supported by statistical techniques for the structural characterization of plastic debris in the marine environment: application to monitoring studies. *Mar. Pollut. Bull.* 106 (1-2), 155–161. doi:10.1016/j.marpolbul.2016.03.012

NHAI (2017). *National highways authority of India, ministry of road transport and highways (2017).* Memo No- 63013/1/2017-18/OTHS/Misc/103/1461.

Murthy, B. S., Latha, R., Tiwari, A., Rathod, A., Singh, S., and Beig, G. (2020). Impact of mixing layer height on air quality in winter. *J. Atmos. Sol.-Terr. Phys.* 197, 105157. doi:10.1016/j.jastp.2019.105157

Nosova, A. O., and Uspenskaya, M. V. (2023). Ecotoxicological effects and detection features of polyvinyl chloride microplastics in soils: a review. *Environ. Adv.* 13, 100437. doi:10.1016/j.envadv.2023.100437

Pérez, I. A., García, M. Á., Sánchez, M. L., Pardo, N., and Fernández-Duque, B. (2020). Key points in air pollution meteorology. *Int. J. Environ. Res. Public Health.* 17 (22), 8349. doi:10.3390/ijerph17228349

Pikis, S., Goldstein, J., and Spektor, S. (2015). Potential neurotoxic effects of polymethylmethacrylate during cranioplasty. *J. Clin. Neurosci.* 22 (1), 139–143. doi:10.1016/j.jocn.2014.06.006

Prata, J. C. (2018). Airborne microplastics: consequences to human health? *Environ. Pollut.* 234, 115–126. doi:10.1016/j.envpol.2017.11.043

Prata, J. C., Reis, V., Matos, J. T., da Costa, J. P., Duarte, A. C., and Rocha-Santos, T. (2019). A new approach for routine quantification of microplastics using Nile Red and automated software (MP-VAT). *Sci. total Environ.* 690, 1277–1283. doi:10.1016/j.scitotenv.2019.07.060

Revell, L. E., Kuma, P., Le Ru, E. C., Somerville, W. R., and Gaw, S. (2021). Direct radiative effects of airborne microplastics. *Nature* 598 (7881), 462–467. doi:10.1038/s41586-021-03864-x

Rodríguez-Seijo, A., and Pereira, R. (2017). Morphological and physical characterization of microplastics. *Compr. Anal. Chem.* 75, 49–66. doi:10.1016/bs.coac.2016.10.007

Roy, A., Mandal, M., Das, S., Popek, R., Rakwal, R., Agrawal, G. K., et al. (2024). The cellular consequences of particulate matter pollutants in plants: safeguarding the harmonious integration of structure and function. *Sci. Total Environ.* 914, 169763. doi:10.1016/j.scitotenv.2023.169763

Shim, W. J., Song, Y. K., Hong, S. H., and Jang, M. (2016). Identification and quantification of microplastics using Nile Red staining. *Mar. Pollut. Bull.* 113 (1-2), 469–476. doi:10.1016/j.marpolbul.2016.10.049

Shruti, V. C., Pérez-Guevara, F., Roy, P. D., and Kutralam-Muniasamy, G. (2022). Analyzing microplastics with Nile Red: emerging trends, challenges, and prospects. *J. Hazard. Mater.* 423, 127171. doi:10.1016/j.jhazmat.2021.127171

Sturm, M. T., Horn, H., and Schuhen, K. (2021). The potential of fluorescent dyes—comparative study of Nile red and three derivatives for the detection of microplastics. *Anal. Bioanal. Chem.* 413, 1059–1071. doi:10.1007/s00216-020-03066-w

Szewc, K., Graca, B., and Dołęga, A. (2021). Atmospheric deposition of microplastics in the coastal zone: characteristics and relationship with meteorological factors. *Sci. Total Environ.* 761, 143272. doi:10.1016/j.scitotenv.2020.143272

Trainic, M., Flores, J. M., Pinkas, I., Pedrotti, M. L., Lombard, F., Bourdin, G., et al. (2020). Airborne microplastic particles detected in the remote marine atmosphere. *Commun. Earth and Environ.* 1 (1), 64. doi:10.1038/s43247-020-00061-y

Van Der Does, M., Knippertz, P., Zschenderlein, P., Giles Harrison, R., and Stuut, J. B. W. (2018). The mysterious long-range transport of giant mineral dust particles. *Sci. Adv.* 4 (12), eaau2768. doi:10.1126/sciadv.aau2768

Veerasingam, S., Ranjani, M., Venkatachalapathy, R., Bagaev, A., Mukhanov, V., Litvinyuk, D., et al. (2021). Contributions of Fourier transform infrared spectroscopy in microplastic pollution research: a review. *Crit. Rev. Environ. Sci. Technol.* 51 (22), 2681–2743. doi:10.1080/10643389.2020.1807450

Wright, S. L., Ulke, J., Font, A., Chan, K. L. A., and Kelly, F. J. (2020). Atmospheric microplastic deposition in an urban environment and an evaluation of transport. *Environ. Int.* 136, 105411. doi:10.1016/j.envint.2019.105411

Yaranal, N. A., Subbiah, S., and Mohanty, K. (2021). Identification, extraction of microplastics from edible salts and its removal from contaminated seawater. *Environ. Technol. and Innovation* 21, 101253. doi:10.1016/j.eti.2020.101253

Yurtsever, M., Kaya, A. T., and Bayraktar, S. Ç. (2018). "A research on microplastic presence in outdoor air," in *Proceedings of the international conference on microplastic pollution in the mediterranean sea.* Editors M. Cocca, E. Di Pace, M. E. Errico, G. Gentile, A. Montarsolo, and R. Mossotti (Cham: Springer), 89–97. doi:10.1007/978-3-319-71279-6

Zhang, Y., Gao, T., Kang, S., Allen, S., Luo, X., and Allen, D. (2021). Microplastics in glaciers of the Tibetan Plateau: evidence for the long-range transport of microplastics. *Sci. Total Environ.* 758, 143634. doi:10.1016/j.scitotenv.2020.143634

Zhang, Y., Kang, S., Allen, S., Allen, D., Gao, T., and Sillanp¨a¨a, M. (2020). Atmospheric microplastics: a review on current status and perspectives. *Earth-Sci. Rev.* 203, 103118. doi:10.1016/j.earscirev.2020.103118

Zhao, S., Danley, M., Ward, J. E., Li, D., and Mincer, T. J. (2017). An approach for extraction, characterization and quantitation of microplastic in natural marine snow using Raman microscopy. *Anal. methods* 9 (9), 1470–1478. doi:10.1039/c6ay02302a

Zhou, Q., Tian, C., and Luo, Y. (2017). Various forms and deposition fluxes of microplastics identified in the coastal urban atmosphere. *Chin. Sci. Bull.* 62 (33), 3902–3909. doi:10.1360/n972017-00956